

# Effects of weak surface fields on the density profiles and adsorption of a confined fluid near bulk criticality

A. Maciołek,<sup>1</sup> R. Evans,<sup>2,3</sup> and N. B. Wilding<sup>4</sup>

<sup>1</sup>*Institute of Physical Chemistry, Polish Academy of Sciences,  
Department III, Kasprzaka 44/52, PL-01-224 Warsaw, Poland*

<sup>2</sup>*H.H.Wills Physics Laboratory, University of Bristol,  
Bristol BS8 1TL, UK*

<sup>3</sup>*Max-Planck-Institut für Metallforschung,  
Heisenbergstr. 3, D-70569 Stuttgart, Germany,*

<sup>4</sup>*Department of Physics, University of Bath  
Bath BA27AY, U.K.*

The density profile  $\rho(z)$  and Gibbs adsorption  $\Gamma$  of a near-critical fluid confined between two identical planar walls is studied by means of Monte Carlo simulation and by density functional theory for a Lennard-Jones fluid. By reducing the strength of wall-fluid interactions relative to fluid-fluid interactions we observe a crossover from behaviour characteristic of the normal surface universality class, strong critical adsorption, to behaviour characteristic of a 'neutral' wall. The crossover is reminiscent of that which occurs near the ordinary surface transition in Ising films subject to vanishing surface fields. For the 'neutral' wall  $\rho(z)$ , away from the walls, is almost constant throughout the slit capillary and gives rise to a  $\Gamma$  that is constant along the critical isochore. The same 'neutral' wall yields a line of capillary coexistence that is almost identical to the bulk coexistence line. In the crossover regime we observe features in  $\rho(z)$  similar to those found in the magnetisation profile of the critical Ising film subject to weak surface fields, namely two smooth maxima, located away from the walls, which merge into a single maximum at midpoint as the strength of the wall-fluid interaction is reduced or as the distance between walls is decreased. We discuss similarities and differences between the surface critical behaviour of fluids and of Ising magnets.

PACS numbers: 64.60.Fr, 05.70.Jk, 68.35.Rh, 68.15.+e

## I. INTRODUCTION

When a fluid, a fluid mixture, a binary alloy or an Ising magnet that is close to a critical point in bulk is brought to a surface its properties are altered significantly. In particular the bulk universality class is divided into several surface universality classes which depend on whether the tendency to order at the surface is increased or decreased w.r.t that in bulk [1,2]. For the case of Ising magnets the phenomenology is well-understood: the critical behavior of the semi-infinite system is governed by a surface scaling field  $c$  which describes the enhancement of interactions in the surface layer.  $c > 0$  corresponds to a reduced tendency to order in the surface and  $c = \infty$  defines the fixed point of the renormalization group transformation of the ordinary transition. Similarly  $c = -\infty$  defines the fixed point for the extraordinary transition and  $c = c^*$  corresponds to the special transition. Such a classification pertains to vanishing (external) surface field  $h_1 = 0$ , a situation which is easily realized for the Ising magnet but not for a fluid; the containing walls must always exert a non-zero surface field of some type. Usually the wall or substrate is assumed to exert an effective potential on the fluid that is infinitely repulsive at short distances and strongly attractive at large distances. Such potentials give rise to pronounced peaks in the density profile of the fluid near the substrate leading to strongly positive adsorption and in magnetic language this corresponds to  $h_1 \gg 0$ . On the other hand, the presence of a substrate should decrease the net fluid-fluid attraction between an atom and its nearest neighbors below the corresponding bulk value so that  $c > 0$ . Thus fluids are expected to lie in the universality class of the normal transition with fixed point  $h_1 = \infty$  and  $c = \infty$ . Since the shapes of the order parameter profiles should be the same whether the symmetry is broken by the external surface field,  $h_1 > 0$ , or spontaneously,  $c < 0$ , the normal and extraordinary transitions should be equivalent [3,4], provided the symmetry breaking fields are sufficiently (infinitely) strong.

In recent years much effort has been focused on understanding the crossover from the normal to the ordinary transition, i.e. the regime of weak surface fields. The length scale associated with the surface scaling field  $h_1$  is  $l_1 \sim h_1^{-\nu/\Delta_1^{ord}}$ , where  $\nu$  is the bulk correlation length exponent and  $\Delta_1^{ord}$  is the surface gap exponent. For a semi-infinite Ising-like system Ritschel and Czerner [5] showed that for small  $h_1$  the order parameter profile can take a

non-monotonic form, increasing with distance  $z$  from the surface for  $z < l_1$  before decreasing for  $z \gtrsim l_1$ . This is quite different from the case of strong field adsorption where the profile decays monotonically, as  $z^{-\beta/\nu}$ , at the critical point. Such behaviour is not predicted by mean-field treatments of Ising systems but was confirmed in several subsequent studies [6–9]; it is also found in exact results for the  $d = 2$  Ising model [10–12]. Physically  $l_1$  corresponds to the distance from the surface over which the order parameter responds linearly with field  $h_1$  [6].

The existence of the critical length scale  $l_1$  has important consequence for *confined* systems near bulk criticality. There are three relevant lengths:  $l_1$ , the distance  $D$  between the two confining surfaces which both exert fields  $h_1$  and the bulk correlation length  $\xi_b$ . Sufficiently close to bulk criticality one can investigate the regime where  $D$  is comparable to  $l_1$  with  $D, l_1 \ll \xi_b$ . In a recent study [13] of the critical  $d = 2$  Ising film order parameter profiles with two symmetric maxima at  $z \sim l_1$  and  $z \sim D - l_1$  were obtained for weak fields  $h_1$ . For even weaker fields when  $l_1 \sim D$  the maxima merge into a single one at midpoint,  $D/2$ . That study provides some of the motivation for the present one where we investigate the density profiles and the Gibbs adsorption for a simple (Lennard-Jones) fluid at bulk criticality that is confined by two planar walls separated by a distance  $D$ . We enquire whether phenomena analogous to these found for Ising systems subject to weak surface fields are found in fluids.

As implied earlier, it is not at all obvious that one can achieve the analogue for a fluid of surface magnetic field  $h_1 \rightarrow 0$ . Thus it is not clear, a priori, that a physical length scale  $l_1$  should exist. On the other hand, one knows that for a purely repulsive wall complete drying with adsorption  $\Gamma \rightarrow -\infty$  (wetting by gas) occurs below the critical temperature  $T_c$  whereas for a strongly attractive wall complete wetting by liquid occurs,  $\Gamma \rightarrow \infty$ , so that one might imagine a scenario whereby for *weak* wall-fluid attraction the adsorption  $\Gamma$  is close to zero. Moreover, if  $\Gamma \approx 0$  for all states on the critical isochore,  $\rho = \rho_c$ ,  $T \geq T_c$ , one might argue that the fluid is exhibiting one of the features of the Ising magnet subject to a vanishing  $h_1$ . In other words, by suitably tuning the wall-fluid potential can one mimic the situation  $h_1 = 0$ , i.e. the ordinary transition? Of course, finding a wall-fluid potential that corresponds *precisely* to  $h_1 = 0$ , i.e., one that generates precisely the same features in the profiles and, therefore, the adsorption for all  $T$ , seems very unlikely - given the lack of Ising symmetry in any 'real' fluid. However, if one does find a wall-fluid potential that is 'neutral', giving rise to  $\Gamma \sim 0$ , then one might also expect to see phenomena associated with small  $h_1$ , i.e. the mesoscopic length scale  $l_1$ . The existence of such phenomena would imply that the ordinary transition is not unique to systems with Ising symmetry and would lend support to the general idea of fluid-magnet universality.

We are not aware of any published proof that a fluid system cannot undergo the ordinary transition [14]. The only rigorous result for fluids [15] is for a planar hard wall where an exact sum rule analysis shows that the surface critical behaviour lies in the universality class of the normal transition and the surface critical exponents can be expressed in terms of bulk critical exponents, as predicted originally in Ref. [3].

What is the experimental situation? To the best of our knowledge there is no experiment that probes critical adsorption in the weak surface field regime for a one-component fluid [16]. For binary fluid mixtures there is strong evidence from (i) reflectivity studies of critical carbon disulphide-nitromethane mixtures adsorbed at a silanated borosilicate glass surface [17] and (ii) ellipsometric studies of an homologous series of critical  $n$  alkane - methyl formate mixtures [18] that the weak adsorption,  $h_1$  small limit, is achieved. In the second of these papers the authors fit their data to a universal scaling function which depends explicitly on  $l_1$  [18]. They argue that as the  $n$  alkane increases from  $n = 11$  to  $n = 14$  the preferentially adsorbed component at the non-critical gas/liquid mixture surface changes from the  $n$  alkane to methyl formate and that this implies an effective surface field  $h_1$  which is small and which changes sign as  $n$  is increased. More specifically they associated  $h_1$  with the difference between the gas-liquid surface energies of the  $n$  alkane and methyl formate in the mixture. In practice this was taken to be the difference between gas-liquid surface tensions of pure  $n$  alkane and pure methyl formate [18]. If  $h_1$  determines whether a particular component is preferentially adsorbed at the interface it is certainly feasible that one can have  $h_1 = 0$ , at least for a certain range of temperatures. However, it is still not clear that a given  $n$  alkane-methyl formate mixture corresponds to a system undergoing an ordinary transition. An earlier reanalysis of surface tension data for isobutyric-acid-water mixtures suggests that the scaling properties are those of a system with a weak surface field, interpreted as the field that determines the preferential adsorption of one component at the non-critical interface [19]. The author also makes the important observation that similar weak-field characteristics should be found at the non-critical interfaces of any binary liquid mixture undergoing a wetting transition close to the critical endpoint [19,20]. For a one-component fluid adsorbed at a solid substrate this situation corresponds to the wetting transition being close to the gas-liquid critical point, a scenario which is expected if the wall-fluid attraction is weak. Crossover between strong and weak-field critical adsorption has been observed in very recent X ray diffraction studies of sublattice order in epitaxial FeCo films grown on an MgO substrate [21]; FeCo undergoes a continuous order-disorder transition from the B2 phase (CsCl structure) to the A2 phase (bcc structure) and the substrate favors (weak) critical adsorption of the B2 phase for  $T \gtrsim T_c$ .

Our paper is arranged as follows: in Sec. II we summarize results for the weak surface field behaviour of Ising systems in the semi-infinite lattice and in film geometry. The magnetization profiles obtained for the latter are directly relevant to our study of a confined fluid. Sec. III reports the results of Monte Carlo simulations of the density profiles and adsorption of the truncated Lennard Jones fluid confined between two planar walls that exert a standard

(10-4) wall-fluid potential. Results are presented at the bulk critical point, and for some states on the critical isochore, for various values of a parameter  $f$  that multiplies the (10-4) potential. By varying  $f$  we tune the strength of wall-fluid interactions relative to fluid-fluid interactions.  $f$  plays a role similar to that of  $h_1$  for the Ising system and for certain values of this parameter we find the system is 'neutral'. This is confirmed by studies of capillary condensation below  $T_c$ . In Sec. IV we describe the results of density functional calculations of the density profiles for the same model system as studied by simulation. By comparing the two sets of results we can assess the role of true surface criticality since the density functional approach is a mean-field one. We conclude in Sec. V with a discussion and summary.

## II. SUMMARY OF RESULTS FOR ISING SYSTEMS

### A. Semi-infinite lattice

We consider an Ising magnet on a semi-infinite lattice with nearest-neighbour pairs of spins interacting (in bulk) with the exchange coupling constant  $J$ . The influence of the surface on the system is usually taken into account by introducing a modified coupling between spins in the surface layer,  $J_1$ , and an (external) surface magnetic field  $H_1 \equiv Jh_1$  imposed on these boundary spins [1,2]. For vanishing bulk magnetic field,  $H \equiv Jh = 0$ , the Hamiltonian of the model reads

$$\mathcal{H} = -J \sum_{\langle ij \rangle \in V} \sigma_i \sigma_j - J_1 \sum_{\langle ij \rangle \in \delta V} \sigma_i \sigma_j - H_1 \sum_{i \in \delta V} \sigma_i \quad (2.1)$$

where  $V$  denotes the volume of the lattice and  $\delta V$  the surface layer. In the absence of the surface field the leading critical behavior of various surface quantities depends on the ratio  $J/J_1$  and is described by three different surface universality classes [1,2]. At the bulk critical point,  $H = 0$ ,  $T = T_c$ , and at the special value  $J_{1c} \simeq 1.50J$  the tendency to order near the surface is unchanged with respect to the bulk. This situation corresponds to the surface universality class of the "special transition". The condition  $J_1 < J_{1c}$  represents the universality class of the "ordinary transition" where the surface has a reduced tendency to order but becomes passively ordered at the bulk phase transition. For  $J_1 > J_{1c}$  spontaneous symmetry breaking also occurs above the critical point and on reducing  $T$  the bulk orders in the presence of an already ordered surface. This situation corresponds to the "extraordinary transition". In the renormalization-group analysis  $J_{1c}$  is an unstable fixed point, whereas for any starting value  $J_1 < J_{1c}$  the surface coupling is driven to the stable fixed point  $J_1 = 0$  by successive renormalization-group transformations. On the other hand, for  $J_1 > J_{1c}$  the coupling is driven to the stable fixed point  $J_1 = \infty$ . In the framework of continuum field theory, appropriate to the universality class of the Ising model, the standard  $\phi^4$  Ginzburg-Landau model is augmented to include the surface by adding the surface contribution:

$$\mathcal{H}_s(\phi) = \frac{1}{2}c\phi^2 - h_1\phi, \quad (2.2)$$

where the parameter  $c$  can be related to the surface enhancement of the spin-spin coupling constant in the lattice models [2]. The leading critical behavior of a semi-infinite system with an ordinary or an extraordinary surface transition is described by stable renormalization-group fixed-point values  $c = +\infty$  and  $c = -\infty$ , respectively. The fixed point for the special transition is at  $c = c^*$ . So far we have not included the effect of the surface field  $h_1$  on the critical system. The presence of the surface field explicitly breaks the order-parameter (OP) symmetry at the surface inducing ordering in the surface layer for  $T \geq T_c$ . It has been argued [3,4] that the extraordinary transition, i.e.  $h_1 = 0$ ,  $J_1 > J_{1c}$  ( $c < c^*$ ), is equivalent to the case with  $h_1 \neq 0$  but with de-enhanced surface couplings:  $J_1 < J_{1c}$  ( $c > c^*$ ). The latter case corresponds to the so called "normal" transition described by the fixed point  $h_1 = \infty$  [4]. The term 'normal' is used because the situation with  $h_1 \neq 0$  and  $J_1 < J_{1c}$  ( $c > c^*$ ) should be generic for simple fluids or fluid binary liquid mixtures bounded by a substrate or wall. Most substrates will attract molecules in a one component fluid giving rise to positive adsorption. Similarly for a binary mixture the substrate will favor one species of the fluid giving rise to preferential adsorption of that species. Both situations correspond to  $h_1 \neq 0$ . Moreover for fluids near walls the number of nearest-neighbor fluid 'bonds' is reduced with respect to the bulk which implies  $J_1 < J_{1c}$  or  $c > c^*$ .

A topic of considerable recent interest concerns the crossover region between the limiting values  $h_1 = \infty$  and  $h_1 = 0$ . At the normal transition the OP (magnetization) profile  $m(z)$  decays monotonically from  $m_1 = 1$  (all spins aligned) at the surface  $z = 0$  to the bulk equilibrium value which is zero for  $T \geq T_c$ , the bulk critical temperature and is nonzero for  $T < T_c$ . At the critical point the decay is described by a universal power law  $m \sim z^{-\beta/\nu}$ , where  $\beta$  and  $\nu$  are the usual bulk exponents, for distances large compared to all length scales. In  $d = 3$  the Ising model exponents give  $\beta/\nu = 0.518(7)$  [22]. By contrast, for  $h_1 = 0$  and  $T \geq T_c$ , at the ordinary transition, the magnetization profile

is zero at any distance from the wall since the OP symmetry is not broken through the whole system [23]. It is of considerable interest to enquire about the profile for small but non-zero  $h_1$ , i.e. in the crossover regime between the ordinary and normal transitions. Mean-field treatments do not predict any interesting behaviour of the magnetization profile;  $m(z)$  starts from a non-zero value  $m_1$  and then decays monotonically to zero [1,3,24,25]. However, as has been shown [5] recently, for small  $h_1$  close to the ordinary transition the critical fluctuations may lead to non-monotonic profiles. Near the surface  $m(z)$  may increase steeply with  $z$  to values much larger than  $m_1$ . Near bulk criticality the range over which this rise occurs depends on  $h_1$  through the length scale induced by this field. In an Ising system near the ordinary transition, i.e. for  $J \ll J_{1c}$ , there is a single relevant surface scaling field  $h_1$  [2] and the length scale induced by this field is  $l_1 \sim h_1^{-\nu/\Delta_1^{ord}}$ , where  $\Delta_1^{ord}$  is the surface gap exponent [26]. At the bulk critical point the magnetization is given by

$$m(z) \sim h_1 z^\kappa \quad \text{for } z \lesssim l_1 \quad (2.3)$$

with  $\kappa = (\Delta_1^{ord} - \beta)/\nu$  [5,7]. In the  $d = 3$  Ising model  $\Delta_1^{ord} > \beta$  and  $\kappa \simeq 0.21$  so  $m(z)$  increases with  $z$  near the surface. For  $z \sim l_1$  the profile has a maximum, and only for  $z \gtrsim l_1$  does crossover to the 'normal' decay  $\sim z^{-\beta/\nu}$  take place. For weak surface fields  $l_1$  can be large (mesoscopic) and thus the increase of the magnetization profile can occur over a mesoscopic distance. In turn, this may influence the behavior of the critical adsorption slightly above  $T_c$  [6,17,18]. The short-distance behavior of the magnetization profile, Eq. (2.3), follows from the critical-point scaling of  $m(z)$  and the (continuity) assumption that  $m(z \rightarrow 0) \sim m_1$ . Since at the ordinary transition the surface layer remains paramagnetic at  $T = T_c$  it should respond linearly to a weak surface field  $h_1$  [3]. The same should hold in the immediate neighbourhood of a surface, thus  $m(z) \sim m_1 \sim h_1$  for  $z \rightarrow 0, h_1 \rightarrow 0$ . Assuming linear response for the scaling function leads to (2.3) [5]. A further heuristic explanation of the short-distance growth of the OP at the ordinary transition was given in Ref. [5,7] on the basis of the behaviour of correlations in the near-surface region. Using scaling analysis and arguments taken from short-distance expansions it was argued that there exists an effective parallel correlation length  $\xi_{\parallel}(z)$  which marks the crossover of the parallel correlation function from "bulk" to "surface" behavior. At  $T = T_c$  the correlations decay algebraically. The decay in planes parallel to the surface is described by  $r^{-d+2-\eta_s}$ , where  $r$  is the distance within the plane parallel to the surface and the exponent  $\eta_s$  depends on the distance  $z$  from the surface. For  $z < l_1$ , in the near-surface region,  $\eta_s$  assumes its bulk value  $\eta$  (slow decay) if  $r \ll z$  whereas for  $r \gg z$ ,  $\eta_s = \eta_{\parallel}^{ord} > \eta$  (fast decay), so we can infer the effective range of correlations  $\xi_{\parallel} \sim z$ . Now assume a weak surface field is imposed at bulk criticality on the surface with  $J_1 \ll J_{1c}$ . The magnetization induced in response at a distance  $z$  from the surface should be proportional to  $h_1$ , to the correlation function in the perpendicular direction describing the decay of the order,  $\langle m(0)m(z) \rangle \sim z^{-d+2-\eta_{\perp}^{ord}}$ , and to the correlated area in the plane parallel to the surface,  $\xi_{\parallel}^{d-1}$ , which can be influenced by a single surface spin. Together these terms give

$$m(z) \sim h_1 \langle m(0)m(z) \rangle \xi_{\parallel}^{d-1} \sim h_1 z^{1-\eta_{\perp}^{ord}} \quad \text{for } z < l_1 \quad (2.4)$$

Scaling relations [7] give in turn  $1 - \eta_{\perp}^{ord} = \kappa$  and we recover (2.3). Many of the above predictions were confirmed by Monte-Carlo simulations for the  $d = 3$  Ising model [8] and by detailed renormalization group studies of a  $\phi^4$  model [7]. Exact results [10–12] and Monte Carlo simulations [9] for the  $d = 2$  Ising model yield magnetization profiles that also increase near the surface for the case of a weak surface field. However, in  $d = 2$  the simple power law (2.3) is modified by a logarithm, i.e.  $m(z) \sim h_1 z^\kappa \log(h_1 z)$ , where  $\kappa = 3/8$ . Note that in mean-field theory  $\Delta_1^{ord} = \beta = 1/2$  so that  $\kappa = 0$  and the magnetisation profile decays monotonically as stated above.

## B. Ising films

In this subsection we consider film geometry, i.e. a lattice of finite width  $D$  in the  $z$  direction but infinite in the other directions. The critical properties of such a confined system should be particularly sensitive to the value of the (identical) surface fields when the length scale  $l_1$  becomes comparable to or larger than the width  $D$ . Recent studies of critical  $d = 2$  Ising films of finite width  $D$  subject to identical surface fields  $h_1 = h_D$  using exact transfer-matrix diagonalization and density-matrix renormalization-group (DMRG) methods fully confirmed this expectation [13]. For weak surface fields such that  $l_1 < D$ , magnetization profiles at  $T = T_c$ ,  $h = 0$  have two symmetric maxima shifted away from the walls and lying at  $z \sim l_1$  and  $z \sim D - l_1$  (see Fig.1). In this regime of  $h_1$  the surface magnetization  $m_1 = m_D$  decreases fairly rapidly as the value of  $h_1$  decreases, whereas the value of the magnetization at the midpoint of the film,  $m(D/2)$ , changes only very slightly. The two separate maxima merge into one, broad maximum located at the middle of the film for smaller  $h_1$  where  $l_1 \sim D$ . For even smaller  $h_1$ ,  $l_1 > D$  and the profiles are nearly flat with the magnetization much lower near the walls than in the central part of the system. In this regime the magnetization

both at the surface and near the midpoint, in fact through the whole profile, decreases as  $\sim h_1 \ln h_1$  (the logarithmic factor is specific to the  $d = 2$  Ising model). This result agrees with the physical interpretation of  $l_1$  as a length scale up to which the OP profile responds linearly (up to the logarithmic factor) to the surface field. Note that the change in the shape of the magnetization profile from one with two maxima to one with a single maximum at the center of a film can be achieved either by decreasing  $h_1$  at fixed  $D$  or by decreasing  $D$  at fixed  $h_1$ . This change is accompanied by a rich variation of the solvation force [13]. The latter is an important thermodynamic quantity characterizing a confined system [27]. For a fluid the solvation force is the excess pressure over the bulk arising from confinement by walls; it can be measured by the surface force apparatus. For the Ising system the solvation force  $= -(\partial f^*/\partial D)_{T,h_1,h}$ , where  $f^*(D)$  is the finite-size contribution to the free energy. The critical-point scaling function of the solvation force, i.e. at  $T = T_c$  and  $h = 0$ , has a pronounced maximum near  $l_1 = D$  (see Fig.6 of Ref. [13]).

### III. SIMULATION STUDIES OF THE LENNARD-JONES FLUID IN A SLIT PORE

In this section we describe the results of a Monte Carlo study of a three dimensional system, namely the truncated Lennard-Jones fluid, confined between two planar walls separated by a distance  $D$ . By decreasing the strength  $f$  of the wall-fluid interactions while keeping the fluid interparticle potential constant we examine the effects of decreased wall-fluid attraction on the shapes of the density profiles and on the form of the adsorption in the critical fluid. Decreasing  $f$  should, in some sense, correspond to reducing  $h_1$  in the Ising system discussed in the previous section.

#### A. Computational details

We have performed Monte Carlo simulations of the Lennard-Jones (LJ) fluid having interparticle interactions of the form:

$$U_{LJ}(r) = 4\epsilon \left[ \left(\frac{\sigma}{r}\right)^{12} - \left(\frac{\sigma}{r}\right)^6 \right]. \quad (3.1)$$

Here  $\epsilon$  measures the well depth of the potential, while  $\sigma$  sets the length scale. The potential was truncated at a radius  $r_c = 2.5\sigma$  and left unshifted. No corrections were applied to account for effects of the truncation. The simulations were performed within the grand canonical (constant- $\mu VT$ ) ensemble [28], permitting fluctuations in the total particle number  $N$ . In order to mimic a slit pore geometry, a cuboidal simulation cell of dimensions  $L_x \times L_y \times D$  (with  $L_x = L_y = L$ ) was employed. Structureless planar walls were imposed in the planes  $z = 0$  and  $z = D$ , while periodic boundary conditions were applied to the cell boundaries in the  $x$  and  $y$  directions parallel to the walls. Fluid particles were assumed to interact with a single planar wall via a long range potential having the form:

$$U_w(z) = 4\epsilon f \left[ \frac{2}{5} \left(\frac{\sigma}{z}\right)^{10} - \left(\frac{\sigma}{z}\right)^4 \right] \quad (3.2)$$

where  $f$  is a parameter that tunes the strength of the fluid-wall interactions relative to those of the fluid interparticle interactions. Decreasing  $f$  simply reduces the depth of the minimum. The total wall-fluid potential is  $U_w(z) + U_w(D - z)$ . We note that  $U_w(z)$  models a wall comprising a single plane of LJ particles [29]. No potential truncation was applied to  $U_w(z)$  since the wall potentials decay considerably less rapidly with increasing separation than the LJ interparticle potential of eq (3.1). Further details of the simulation procedure are given in an earlier study [30]. In the course of the simulations the one-dimensional density profile was accumulated:

$$\rho(z) \equiv \int_0^L \rho(\mathbf{r}) dx dy, \quad (3.3)$$

representing the configurationally averaged local number density at a given distance  $z$ . Measured forms of this profile for a range of wall strengths  $f$  at the liquid-gas critical point and along the critical isochore are presented in the following subsection.

#### B. Density profiles at the critical point

The bulk critical point parameters of the truncated LJ fluid have previously been determined from an accurate finite-size scaling study [31]. They are (in standard reduced LJ units [28]),  $T_c = 1.1876(3)$ ,  $\mu_c/k_B T_c = -2.778(2)$ .

Using these parameter values we have obtained the density profiles  $\rho(z)$  for a range of wall strengths  $f$ . The results for a system of size  $L = 15\sigma, D = 40\sigma$  are shown in Fig. 2(a). A magnified plot of the region around the critical density  $\rho_c = 0.3197(4)$  (horizontal line) is shown in Fig. 2(b). Examination of the profiles of Fig. 2 reveals three qualitatively distinct regimes of behaviour as the wall strength  $f$  is varied. We discuss them in turn. For the smallest values of  $f$  studied, the density near the wall lies well below its critical value and the profile exhibits little structure. Moving away from the wall, however, the density increases, reaching a maximum in the slit middle, although it at no stage attains the bulk critical value. The overall shape of the profile is convex upwards with respect to the critical density. For the largest values of  $f$  studied, the density near the wall is much higher than the critical density and large packing effects are evident in the profile. As the distance from the wall increases, the density falls progressively, although it does not reach the bulk value. The profile is convex downwards with respect to the critical density. For intermediate values of  $f$ , the packing-induced density oscillations near the wall span the critical density, while further away from the wall the magnitude of the profile curvature is generally less than in the large or small  $f$  limits. A magnified view of the region around the critical density is given in Fig. 2(b). Strikingly there exist some  $f$  values in this regime for which  $\rho(z)$  exceeds  $\rho_c$ , but the profile is *concave upwards* with respect to the critical density. Thus  $\rho(z)$  exceeds  $\rho_c$  and *increases* with increasing distance from the wall. As  $f$  increases, however, one sees (Fig. 2(c)) the formation of a structure with two smooth maxima in the profile, the maxima being some distance from the walls. On further increasing  $f$ , the maxima become more pronounced and their positions move closer to the walls. Clearly these results show very similar features to the magnetisation profiles shown in Fig.1. It is also instructive to observe the effect of changing the slit width on the double maxima profile of Fig. 2(c). The comparison with a profile for a slit of width  $D = 20\sigma$  is made in Fig. 3, from which one sees that the double maxima profile is replaced by one with a single maximum in the narrower slit. Once again this is similar to what is found for the Ising system (Sec. II).

### C. Properties of the Neutral Wall System

The results of the last subsection suggest that for certain choices of the strength parameter  $f$  the confined Lennard-Jones fluid is behaving similarly to an Ising film with  $h_1 \approx 0$ . Density profiles for  $f \lesssim 0.653$  are of particular interest since it is in this regime of  $f$  that there is a crossover from a maximum to a minimum in the profile at the midpoint.

One of the signatures of the ordinary transition (at a single surface) is that the magnetisation profile remains constant,  $m_l = 0, l = 1, 2, \dots$  for all  $T \geq T_c$  and  $h = 0$ . The analogous situation for a confined fluid should be  $\rho(z) = \rho_c$ , the critical density, except for distances close to the wall where packing constraints induce oscillations in the profile, for states on the critical isochore:  $\rho_{bulk}(\mu, T) = \rho_c, T \geq T_c$ . This implies, in turn, the adsorption  $\Gamma = \int_0^D (\rho(z) - \rho_c) dz$  should be constant (and close to zero) along the critical isotherm.

We varied  $f$  in an attempt to find a 'neutral' wall where such properties were achieved. Figs 4(a) and 4(b) display the density profiles on the critical isochore for  $f = 0.644, D = 40\sigma$  and  $20\sigma$ , respectively. In each case the density profile is almost flat throughout the slit except for near the walls. Fig.5 shows a plot of the adsorption  $\Gamma\sigma^2$  versus  $\tau = (T - T_c)/T_c$  for  $D = 20\sigma$  and a selection of values of  $f$ . We observe that  $\Gamma$  is temperature independent for the 'neutral' wall with  $f = 0.644$ . Increasing  $f$  slightly leads to positive adsorption near  $T_c$  whereas decreasing  $f$  below 0.644 leads to more pronounced negative adsorption which is  $T$  dependent.

Note that the simulations were performed at chemical potentials  $\mu$  measured along the critical isochore of the bulk fluid. These were determined, using periodic boundary conditions, in Ref. [30].

Further evidence that  $f = 0.644$  corresponds to a 'neutral' wall is furnished by considering the confined fluid *below*  $T_c$ . For strongly attractive walls, favouring the liquid phase, we expect liquid-gas coexistence to occur at a chemical potential  $\mu$  which lies below the value  $\mu_{cx}$  for bulk coexistence at the same temperature [27] whereas for purely repulsive walls, favouring gas, coexistence should occur at a higher value than in bulk. We determined the line of capillary coexistence, where liquid and gas coexist, in the slit with  $D = 20\sigma$ . For  $-0.1 < \tau < 0$  and  $f = 0.644$  we found this line was hardly shifted from the bulk coexistence line - see Fig. 6. The greatest deviation, at  $\tau = -0.1$ , was about 0.1%, with condensation in the slit occurring for a (slightly) higher value of  $\mu$ , implying the walls with  $f = 0.644$  favor (slightly) the gas phase, i.e. the contact angle is (slightly) larger than  $\pi/2$  at this temperature [27]. The inset to Fig. 6 displays the difference between the chemical potential  $\mu$ , for capillary coexistence, and the corresponding value  $\mu_{cx}$ , for bulk coexistence, for three values of  $f$ . One observes that for  $f = 0.71, \mu - \mu_{cx}$  remains substantially more negative than the result for  $f = 0.644$  whereas for  $f = 0.59$ , corresponding to a weaker wall attraction,  $\mu - \mu_{cx}$  is positive at all temperatures in the range considered. These results suggest that a value of  $f$  slightly lower than 0.644 would yield capillary coexistence very close to that in bulk, i.e. would correspond in magnetic language to a surface field  $h_1 = 0$  as regards the phase behaviour below  $T_c$ .

#### IV. DENSITY-FUNCTIONAL THEORY STUDIES OF THE LENNARD-JONES FLUID IN A SLIT PORE

Having established that computer simulations of the critical Lennard-Jones fluid do find features in the density profile that mimic those found for the magnetisation profile in systems with weak surface fields  $h_1$ , we now enquire whether any of these features are also found in a mean-field treatment of the same confined fluid. The oscillations in the profiles shown in Figs 2-4, arise from packing effects near the walls and these should certainly be captured by a suitable density functional theory (DFT) approach. Recall, however, the double maxima, separated by a shallow minimum, is a feature which reflects true surface criticality in the case of a magnetic system (Sec. II). Does the presence of a similar feature in the simulation results for fluids also signal some manifestation of surface criticality or is the feature somehow reflecting the particular form of the wall-fluid potentials? By carrying out mean-field calculations we attempt to address these questions.

We consider the same system of particles as in Sec. III, i.e. the Lennard-Jones fluid with the pair potential given by (3.1), but *not* truncated, and apply the DFT [32] to determine the density profile at the bulk critical point. All the functionals implemented here are of mean-field type; bulk critical exponents would take their mean-field values. We assume that the fluid is confined between two identical parallel walls located at  $z = 0$  and  $z = D$ , and infinite in the  $x$  and  $y$  directions. As previously, the system is in contact with a reservoir of fluid at temperature  $T_c$  and critical chemical potential  $\mu_c$ . The grand potential of the inhomogeneous system is a functional of the one-body density distribution  $\rho(\mathbf{r})$  [32]:

$$\Omega[\rho] = \mathcal{F}[\rho] - \int d\mathbf{r}(\mu - V(\mathbf{r}))\rho(\mathbf{r}), \quad (4.1)$$

where  $V(\mathbf{r}) \equiv V(z)$  is the total wall-fluid external potential and the equilibrium density profile  $\rho(\mathbf{r}) \equiv \rho(z)$  corresponds to the minimum of  $\Omega[\rho]$ . The simplest form for  $\Omega[\rho]$  which should be appropriate near criticality is based on the square gradient approximation to the intrinsic Helmholtz free energy functional  $\mathcal{F}[\rho]$  with the wall-fluid contribution modeled by a term  $\Phi_s$  which depends only on the fluid density at contact i.e.  $\Phi_s = \frac{c}{2}(\rho^2(0) + \rho^2(D)) - \varepsilon_w(\rho(0) + \rho(D))$ , where  $c$  and  $\varepsilon_w$  are constants characterizing the effects of the wall. Although functionals of this type cannot incorporate short-ranged correlations arising from packing and hence cannot account for the oscillatory behavior of the density profile near the walls [27], they were successfully employed in studies of finite size effects on the critical adsorption in large pores, as this phenomenon is dominated by the slow decay of the profile far from the walls [33,30]. However, the density profiles obtained from this approximation are always monotonic; depending on the value of  $c$  and  $\varepsilon_w$ ,  $\rho(z)$  is either monotonically increasing or monotonically decreasing. This observation follows straightforwardly from the graphical construction for the solution of the Euler-Lagrange (differential) equation [33,34] and remains valid for the local functional approach employed by Borjan and Upton [35] in their studies of a critical confined system. Thus it is necessary to consider other approximations for the intrinsic free energy functional [32,36], in which  $\mathcal{F}[\rho]$  is divided into contributions to the free energy functional arising from repulsive forces,  $\mathcal{F}_r[\rho]$ , and from the attractive part of the pairwise potential; the latter is treated in mean-field or random-phase approximation. Using hard-spheres (HS) as the reference fluid one constructs a Van der Waals approximation:

$$\mathcal{F}[\rho] = \mathcal{F}_{HS}[\rho] + \frac{1}{2} \int d\mathbf{r}_1 \int d\mathbf{r}_2 \rho(\mathbf{r}_1)\rho(\mathbf{r}_2)\phi_{att}(r_{12}), \quad (4.2)$$

where  $r_{12} = |\mathbf{r}_1 - \mathbf{r}_2|$ . The attractive part of the pairwise potential is not specified uniquely. Here we employ the prescription:

$$\begin{aligned} \phi_{att} &= U_{LJ}(r_0) & r \leq r_0 \\ &= U_{LJ}(r) & r > r_0, \end{aligned} \quad (4.3)$$

where  $r_0 = 2^{1/6}\sigma$  is the minimum of the LJ potential and  $U_{LJ}(r_0) = -\epsilon$ . In this approximation the Helmholtz free energy density of a uniform fluid has the form:

$$f(\rho) = f_{HS}(\rho) - \frac{\rho^2}{2}\alpha, \quad (4.4)$$

with  $\alpha = -\int d\mathbf{r}\phi_{att}(r) > 0$ . For simplicity we set the hard sphere diameter  $d$  equal to  $\sigma$ . We describe results of calculations using both the weighted density approximation (WDA) and the local density approximation (LDA) for  $\mathcal{F}_{HS}[\rho]$  [36].

## A. Results from WDA

In order to incorporate correctly the main features of the short-range structure of a fluid near the walls, we employ a simple non-local approximation for  $\mathcal{F}_{HS}[\rho]$  based on the weighted-density approximation [37–39]:

$$\mathcal{F}_{HS}[\rho] = \mathcal{F}_{id}[\rho] + \int d\mathbf{r} \rho(\mathbf{r}) \psi_{ex}(\bar{\rho}(\mathbf{r})), \quad (4.5)$$

where the ideal gas contribution is

$$\mathcal{F}_{id}[\rho] = \int d\mathbf{r} \rho(\mathbf{r}) [\ln(\Lambda^3 \rho(\mathbf{r})) - 1]. \quad (4.6)$$

$\Lambda$  is the thermal de Broglie wavelength.  $\psi_{ex}$  is the excess, over ideal, of the free energy per particle of the uniform fluid. In (4.5) this quantity is calculated at some weighted density  $\bar{\rho}$ , where  $\bar{\rho}$  is a non-local functional of the true density  $\rho$  obtained by taking the weighted average of  $\rho(\mathbf{r})$  over a local volume reflecting the range of interatomic forces:

$$\bar{\rho}(\mathbf{r}) = \int d\mathbf{r}' \rho(\mathbf{r}') w(|\mathbf{r} - \mathbf{r}'|). \quad (4.7)$$

The precise definition of  $w$  depends on the particular version of WDA; the most sophisticated versions introduce weight(s) so that the second functional derivative of  $\mathcal{F}_{HS}[\rho]$  reproduces the two-particle direct correlation function  $c^{(2)}(r)$  of a uniform hard sphere fluid [36]. In this paper we assume the simplest, density independent step function form for  $w(r)$ , i.e.  $w(r) = 3/(4\pi d^3) \Theta(d - r)$ , where  $\Theta(x)$  denotes the Heaviside step function. This choice yields reasonable results for the density profiles near a hard wall [38]. The excess free energy per atom is given by the Carnahan-Starling expression:

$$\psi_{ex}(\rho) = k_B T \frac{\eta(4 - 3\eta)}{(1 - \eta)^2}, \quad (4.8)$$

where  $\eta = \frac{1}{6} \pi \rho d^3$  is the packing fraction. Minimizing  $\Omega[\rho]$  in (4.1) with the external potential  $V(z)$  yields an integral equation for the density profile of the fluid:

$$\begin{aligned} \rho(z) = & \rho_0 \exp\left\{-(1/k_B T) [\psi_{ex}(\bar{\rho}(z)) + \int d\mathbf{r}' \rho(z') \psi'_{ex}(\bar{\rho}(z')) w(|\mathbf{r} - \mathbf{r}'|) \right. \\ & \left. + \int d\mathbf{r}' \rho(z') \phi_{att}(|\mathbf{r} - \mathbf{r}'|) + V(z)]\right\}, \end{aligned} \quad (4.9)$$

where  $\rho_0 = \Lambda^3 \exp(\mu/k_B T)$ .

We solve this equation numerically for two choices of the single wall potential  $U_w(z)$ : (a) a long range potential with the same form used in simulations (3.2) and (b) a hard wall potential with an attractive short-ranged tail:

$$\begin{aligned} U_{ws}(z) = & \infty & z < 0 \\ = & -\epsilon f \exp(-z/\sigma) & z > 0. \end{aligned} \quad (4.10)$$

Once again the strength parameter  $f$  determines the depth of the potential well. The integral equation (4.9) was solved using a minimization procedure [40] which, in principle, is always convergent; the commonly used iteration is much less efficient near bulk criticality where profiles decay very slowly. We minimize the function

$$u(\rho_1, \dots, \rho_N) = \sum_{i=1}^N (\rho_i - \tilde{\rho}_i)^2, \quad (4.11)$$

where  $\rho_i = \rho(z_i)$  are densities calculated at  $N$  points between  $z = 1$  and  $z = D$  and are treated as independent variables.  $\tilde{\rho}_i$  denotes the right-hand side of the integral equation (4.9) calculated at  $z = z_i$ ;  $\tilde{\rho}_i$  are functions of  $\rho_i$ , i.e.  $\tilde{\rho}_i = \tilde{\rho}_i(\rho_1, \dots, \rho_N)$ . The minimum  $u \approx 0$  corresponds to the solution of (4.9). This minimum is determined using the conjugate gradient method. Calculations were performed for the slit pore of the same width as in the simulations,  $D = 40\sigma$ , at the critical point of the uniform fluid. The mean field free energy density (4.4) gives, for our model,  $k_B T_c/\epsilon = 1.00617(2)$  and  $\rho_c \sigma^3 = 0.24912(4)$ . To allow for the expected oscillatory behavior of the profile near the walls we used a very fine mesh,  $N = 400$ . As a starting density profile we usually took  $\rho(z) = \rho_c$ .



In Fig.7(a) we show density profiles obtained for the long-ranged wall-fluid potential (3.2) for various strengths  $f$  between 0 and 1. The sequence of profiles is very similar to that obtained in simulations (see Fig. 2(a)), i.e. there are three different types of profile shape depending on the value of  $f$ . For the smallest values of  $f$  studied (between 0 and about 0.55), the profiles are convex upwards with respect to  $\rho_c$  and exhibit little structure, whereas for the largest values of  $f$  studied (between about 0.7 and 1) the profiles are convex downwards with  $\rho(z) > \rho_c$  and show very pronounced oscillations near the walls. At intermediate values, i.e. as  $f$  increases above  $\approx 0.55$  the profiles become flatter in the central part of the slit. They remain concave upwards with respect to the critical density but move as a whole towards greater values so that except near the walls,  $\rho(z) > \rho_c$  - see Fig. 7(b). A difference between results from the WDA and those from simulations occurs when the two smooth maxima, separated by a shallow minimum, structure forms in the profile. In the simulations these new maxima are more pronounced than in WDA and are located somewhat closer to the walls. It is instructive to compare the height and position of the new maxima with those of the third peak in the density profile, arising from packing effects (layering) near the walls. In the WDA this third peak is located at  $z \approx 3\sigma$ . For  $f \lesssim 0.55$  the peak is not pronounced indicating weak packing effects in the weakly attractive wall potential. As  $f$  is increased the third peak becomes more pronounced and the value of the density at this peak increases rapidly. For  $f \lesssim 0.63$  this density lies below the density at the midpoint,  $\rho_{mid}$ , and below the density at the new maxima (where these have developed). However for  $f$  in the range  $0.63 \lesssim f \lesssim 0.64$  the density in the region of the third peak grows more rapidly than in the central portion of the density profile and for  $f \gtrsim 0.64$  the density at the third peak is higher than at the new maxima and  $\rho_{mid}$ . The positions of the new maxima move closer to the walls as  $f$  increases and for  $f \gtrsim 0.68$  these maxima cannot be discerned. Note that the range of values of  $f$  corresponding to the three qualitatively different regimes of behavior of the profile are very close to those found in simulations.

In Fig. 8 we plot the adsorption  $\Gamma\sigma^2$  versus  $\tau$ , for  $D = 40\sigma$ , calculated along the critical isochore  $\rho = \rho_c$ , for several values of  $f$ . These results should be compared with those from simulation in Fig. 5 noting that the latter correspond to a *much* wider range of the strength parameter  $f$ . We should also note the difference in vertical scale between these two figures; the adsorption is very weak within the WDA for the narrow range of  $f$  displayed in Fig. 8. On the basis of this figure we might conclude that a value of  $f$  in the range  $0.561 \lesssim f \lesssim 0.564$  corresponds to a 'neutral' wall. In this range  $\Gamma$  changes from monotonically increasing with  $\tau$  to exhibiting a shallow minimum. There is some value for which  $\Gamma(\tau)$  is flat and negative, c.f. Fig. 5.

Figure 9(a) presents a selection of the profiles calculated for the short-ranged wall-fluid potential (4.10) with various strengths  $f$  between 1 and 0. There are generally fewer oscillations near the walls and the contact values  $\rho(0) = \rho(D)$  are large for large values of  $f$  but away from the walls the shape of the profile changes in a similar way as for the long-ranged  $U_w(z)$  as  $f$  is increased. The two smooth maxima structure forms at much larger values of  $f$  however, i.e., at about 0.8 and then shifts rapidly towards the walls, merging with oscillations - see Fig.9(b). Such behaviour might reflect the narrower attractive well in the wall-fluid potential. One requires a larger  $f$  to acquire the same strength of attraction. In the range of  $f$  we studied there are no profiles characteristic of strongly adsorbing walls with extreme packing effects.

## B. Results from LDA

In the local density approximation (LDA) the free energy functional of the hard-spheres has a form:

$$\mathcal{F}_{HS}[\rho] \approx \int d\mathbf{r} f_{HS}(\rho(\mathbf{r})), \quad (4.12)$$

where  $f_{HS}(\rho)$  is the Helmholtz free energy density of a uniform hard-sphere fluid with density  $\rho$  [32,36]. The LDA does not incorporate the short-ranged correlations that characterize the structure of dense liquids and hence it cannot describe oscillatory profiles arising from packing effects. Attractive interparticle forces are still treated by the mean-field approximation given in (4.2) and the free energy density of the uniform fluid is still given by (4.4) so that the critical point remains the same as that given in the previous subsection.

Critical point profiles for the slit of width  $D = 40\sigma$  obtained in the LDA for the long-ranged wall-fluid potential (3.2) are shown in Fig. 10(a). The wall strengths  $f$  are the same as in Figs.9. Despite the very crude approximation, some weak structure remains in the profiles. The sequence of profiles is reminiscent in shape to those from Fig. 9, i.e. for WDA with the short-ranged wall-fluid potential. For  $f < 0.8$  the shapes are convex upwards with respect to the critical density and, except for the first peak near the walls,  $\rho(z)$  lies below  $\rho_c$ . Profiles for  $f \geq 0.8$  are similar in shape to these obtained in simulation and in WDA for intermediate values of  $f$  - see Fig. 10(b). As was the case for WDA with the short-ranged wall-fluid potential, the characteristic two smooth maxima structure is formed for larger values of  $f$  than in simulations.

## V. DISCUSSION

In this paper we have performed extensive Monte Carlo simulations and density functional calculations of the density profile and Gibbs adsorption  $\Gamma$  for a Lennard-Jones fluid confined between two planar walls under conditions where the reservoir is at, or close to, bulk criticality. We observe that increasing the parameter  $f$  that multiplies the (10-4) wall-fluid potential alters the profile dramatically, from one typical for a purely repulsive wall ( $\Gamma$  is strongly negative) to one typical of a strongly attractive wall ( $\Gamma$  is strongly positive), for the critical fluid at fixed wall separation  $D$ . In the simulations we find that for  $f \approx 0.644$  the confined LJ fluid behaves in a similar fashion to an Ising film with vanishing surface field  $h_1 = 0$ , i.e. to what is observed at the ordinary transition. This 'neutral' wall scenario is characterized by a fluid density profile which, away from the walls where oscillations arise, is almost constant throughout the slit and which gives rise to a  $\Gamma$  that is constant along the critical isochore (see Figs 4 and 5). The same value  $f \approx 0.644$  gives rise to a line of capillary coexistence for  $T < T_c$  that differs very little from the bulk coexistence line (see Fig. 6), supporting the contention that this value corresponds to a 'neutral' wall. Moreover, we observe that as  $f$  decreases from 1 the density profile of the critical LJ fluid, away from the walls, exhibits features reminiscent of those found for the magnetisation profile of the critical Ising film in the crossover regime between the 'normal' and ordinary surface universality classes which is achieved by reducing the surface field  $h_1$  towards zero. In particular for  $0.7 \gtrsim f \gtrsim 0.64$  and  $D = 40\sigma$  we find profiles with two smooth maxima, located away from the walls; compare Figs 2b and 1. As  $f$  is reduced further, or as the slit width  $D$  is reduced at fixed  $f$ , these maxima merge into a single maximum located at the midpoint  $D/2$ . In the Ising film a magnetisation profile with two smooth maxima is characteristic of a system subject to weak surface fields  $h_1 = h_D$ ; the profile increases for distances  $z \lesssim l_1 \sim h_1^{-\nu/\Delta_1^{ord}} < D/2$ , before decaying to the value at the midpoint (see Sec. II). For weaker  $h_1$  (or smaller  $D$ ) a single maximum forms at the midpoint when  $l_1 \sim D/2$ .

In the light of the simulation results it is tempting to argue that the near critical LJ fluid does exhibit several features in common with the Ising system. Consideration of the adsorption and of capillary condensation would suggest identifying  $h_1 = f - f_{neutral}$ , with  $f_{neutral} \approx 0.644$ . However, the fluid density profiles at the critical point clearly do not exhibit the symmetry  $m(z; -h_1) = -m(z; h_1)$  of the magnetisation profile of the Ising system - even when some attempt is made at coarse graining the oscillations near the walls and subtracting a constant density. Thus it is not obvious what is the best choice of order parameter profile for the fluid. The form of the confining potential obviously plays an important role and in order to investigate this further we performed a series of DFT calculations using a very simple WDA to incorporate short-ranged correlations.

Our DFT results also point to the existence of a 'neutral' wall; the adsorption  $\Gamma(\tau)$  calculated along the critical isochore is almost flat for  $f$  lying between 0.561 and 0.564 pertaining to the same (10-4) wall potential and wall separation  $D = 40\sigma$  as the simulations - see Fig. 8. Moreover, the DFT density profiles exhibit the characteristic two smooth maxima for an intermediate range of  $f$  observed in the simulations - see Fig. 7. What does this lead us to conclude about the role of critical fluctuations in determining the shape of the density profiles for 'weak' surface fields? Recall that unlike simulations DFT is a mean-field treatment which does not incorporate effects of fluctuations. The critical scaling arguments of Sec. II state categorically that the mean field order parameter profile for the Ising system subject to a surface field  $h_1$  acting on the surface layer only should vary monotonically away from the wall, i.e. there should be no maxima. The mean-field value of the exponent that describes the short-distance behaviour of the profile, Eq. (2.3), is  $\kappa = 0$ . That we find smooth maxima in the density profiles within our DFT treatment would seem to reflect the shape of the confining (wall-fluid) potential. Note that the precise form of wall-fluid potential is not crucial as we also find the maxima, albeit for larger values of  $f$ , for a short-ranged, exponentially decaying attractive potential - see Fig. 9. There are quantitative differences between DFT and simulation. The maxima are more pronounced, are located closer to the walls and appear to shift faster towards the midpoint as  $f$  is decreased in simulation and this might reflect the presence of fluctuation effects. The latter give rise to a slightly higher value of the exponent determining the length scale  $l_1 \sim h_1^{-\nu/\Delta_1^{ord}}$  than in mean field, i.e. the  $d = 3$  Ising value is 1.3 rather than 1. These observations suggest that one should re-analyse the arguments which lead to Eq. (2.3). Both arguments given in Sec. IIA are based on the assumption that the surface magnetisation  $m_1$  and  $m(z \sim 0)$  respond linearly to a weak  $h_1$  for  $T = T_c$ . Whilst this is eminently plausible for the Ising system it is not clear how to translate to the case of a fluid near a wall. It is possible that the shape of the external potential has non-trivial repercussions for the short-distance expansion of the order parameter profile. However, one should also bear in mind that there is a further complication in attempting to relate crossover behaviour in fluids to that in systems with Ising symmetry. The reduced order parameter symmetry of bulk fluids lead to scaling field mixing [41,42]. However, to our knowledge, there have to date been no considerations of the consequences of this reduced symmetry in the context of surface critical behaviour of fluids. Any scaling theory that seeks to encompass fluid and magnet surface critical behaviour within a unified description must address this issue.

One way of doing so may be to generalize the role of the surface scaling fields  $c$  and  $h_1$  (defined for Ising-like

systems) such that regardless of the model system, they correspond to equivalent paths in the surface phase diagram. Consider the case of an Ising model in zero bulk field at its bulk critical temperature. Within the surface phase diagram, the line  $h_1 = 0$  corresponds to a special symmetry line of the system because the magnitude of the surface order parameter is invariant with respect to a change of sign of  $h_1$ . The scaling field  $c$  (which relates to missing neighbours and surface induced modifications of surface couplings), controls the temperature at which the surface orders relative to the bulk. The sign or magnitude of  $c$  does not determine which phase is preferred at the wall, thus the  $c$  field can be represented as a vector coincident with the symmetry line  $h_1 = 0$  (Fig. 11(a)).

By contrast in a fluid, missing neighbours typically lead to a segregation of one phase to the wall, i.e. to breaking of the order parameter symmetry with respect to its bulk critical point value. In terms of the geometrical picture outlined above, the line of surface order parameter symmetry lies off-axis in the surface phase diagram and does not coincide with the  $c$ -field. In attempting to restore the symmetry, one might consider applying a non-zero external surface field  $h_1$  that couples to the order parameter near the surface, and whose magnitude is chosen such as to return the value of the order parameter at the surface to its bulk critical value. Within this framework, the combined  $c$  and  $h_1$  fields can be regarded as an *effective* field  $\tilde{c}$  directed along the symmetry line. Similarly we require an effective field  $\tilde{h}_1$  (the scaling equivalent to the Ising model  $h_1$ ) which measures deviations from this line (Fig. 11(b)). Formally these ends can be attained by introducing ‘mixed’ surface fields having the form

$$\begin{aligned}\tilde{c} &= (c - c^*) + a_1 h_1 \\ \tilde{h}_1 &= h_1 + a_2 (c - c^*),\end{aligned}\tag{5.1}$$

with  $a_1$  and  $a_2$  system specific constants (both zero in the Ising model context) whose values control the degree of field mixing.

The starting point for exploring the consequences of field mixing for surface critical behaviour is an expression for the singular part of the surface free energy. In terms of the mixed fields this is

$$F_{sur}^s \approx \tilde{\tau}^{2-\alpha} f_{sur}^\pm(\tilde{\mu}\tilde{\tau}^{-\Delta}, \tilde{c}\tilde{\tau}^{-\phi}, \tilde{h}_1\tilde{\tau}^{-\Delta_1}),\tag{5.2}$$

where  $f_{sur}^\pm$  denote scaling functions, while  $\tilde{\tau}$  and  $\tilde{\mu}$  are (mixed) bulk scaling fields which in the Ising context reduce to the reduced temperature and reduced bulk field respectively [42]. The positive constants  $\Delta$  and  $\Delta_1$  are respectively the gap exponent and surface gap exponents, while  $\phi$  is an exponent controlling the crossover from the ordinary to the normal universality classes.

We shall not attempt to explore the consequences of surface field mixing in any great depth here, although we do hope to report on the matter in future work. For the time being, we merely point out that one corollary of Eq.(5.2) is that—in a simple fluid—the scaling equivalent of the Ising model magnetisation profile  $m(z)$  is not the density profile  $\rho(z)$ , but a profile formed by linearly combining the density and the energy density profiles. One should also consider the adsorption not on the critical isochore, but on an analytical extension of the coexistence diameter. These observations may prove important in exposing more fully the universality of surface critical phenomena for fluids and magnets.

Finally, with regard to the applicability of the above considerations to realistic fluids, the question arises as to just what constitutes the surface field  $h_1$  in a fluid. Clearly the wall-fluid potential in general couples to the order parameter in the vicinity of the surface and thus can be used to tune its value. However, as noted in Sec. I, a realistic potential such as the 10-4 potential used in this work will not allow one to restore the order parameter to its bulk critical value exactly at all distances from the wall. Short ranged packing effects will always be visible close to the wall. Nevertheless, in the context of the ordinary transition, the length scale on which packing effects occurs will be negligible compared to the length scale of the critical phenomena (set by  $l_1$ ). Hence one might speculate that fluid-magnet universality should be evident provided one views the system on sufficiently large length scales, i.e. such that the value of a suitably *coarse-grained* order parameter profile matches its bulk value near the wall.

## ACKNOWLEDGMENTS

We have benefited from conversations with A. Ciach, S. Dietrich, M. Krech, B. M. Law, A. O. Parry, F. Schlesener and, in particular, P. J. Upton. R. E. is grateful to S. Dietrich and his colleagues at MPI Stuttgart for their hospitality and to the Alexander von Humboldt Foundation for financial support under GRO/1072637. This work was supported by Royal Society travel grants and partially by KBN (grant no. 4 T09A 066 22).

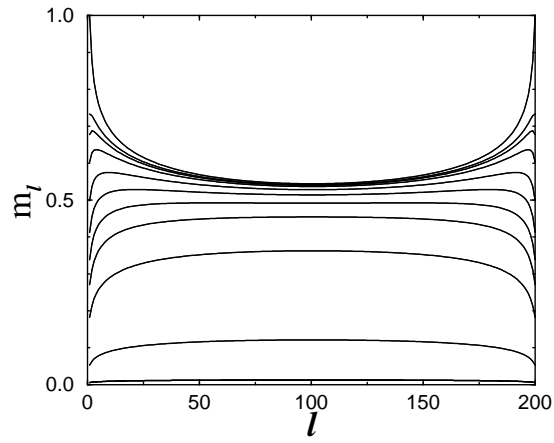
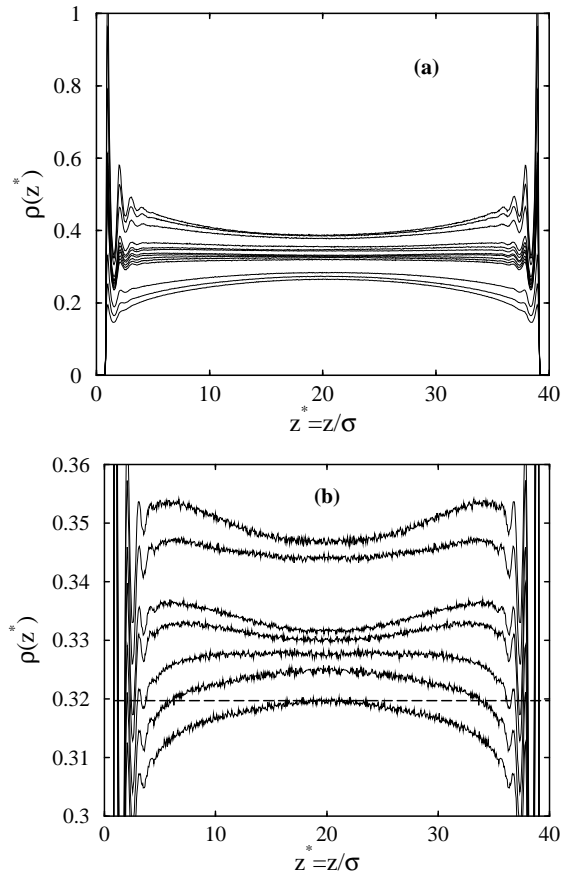


FIG. 1. Magnetization profiles  $m_l$  of the  $d = 2$  Ising film of width  $D = 200$  lattice spacings for  $T = T_c$  and zero bulk field and several values of the surface field  $h_1 = h_D$ : from top to bottom profile:  $h_1 = 10, 0.5, 0.4, 0.3, 0.2, 0.14, 0.1, 0.07, 0.04, 0.01, 0.001$ . These results were obtained using exact transfer-matrix diagonalization (adapted from Ref. 13).



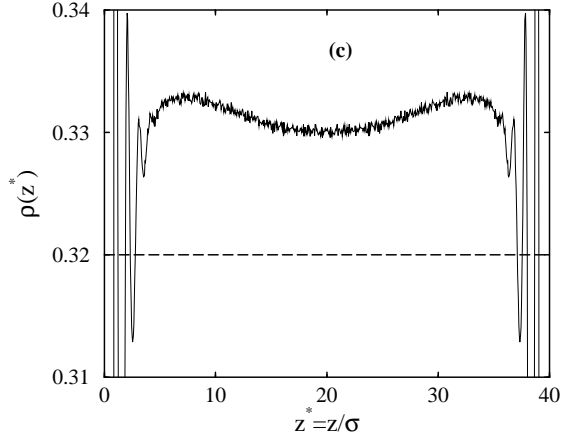


FIG. 2. **(a)** The measured critical point density profiles  $\rho(z)$  (in units of  $\sigma^3$ ) for a LJ system of size  $L = 15\sigma$  and width  $D = 40\sigma$ . Wall strengths  $f$  from top to bottom:  $f = 1.0, 0.9, 0.8, 0.7, 0.68, 0.67, 0.66, 0.653, 0.64, 0.63, 0.62, 0.5, 0.4, 0.3$ . The horizontal dashed line denotes the bulk critical density,  $\rho_c = 0.3197(4)$  **(b)** Magnified version of (a) showing the region close to the critical density. Wall strengths  $f$  from top to bottom:  $f = 0.68, 0.67, 0.66, 0.653, 0.64, 0.63, 0.62$ . **(c)** Magnified version of the profile for  $f = 0.653$  showing the two smooth maxima with a shallow minimum in the centre of the slit.

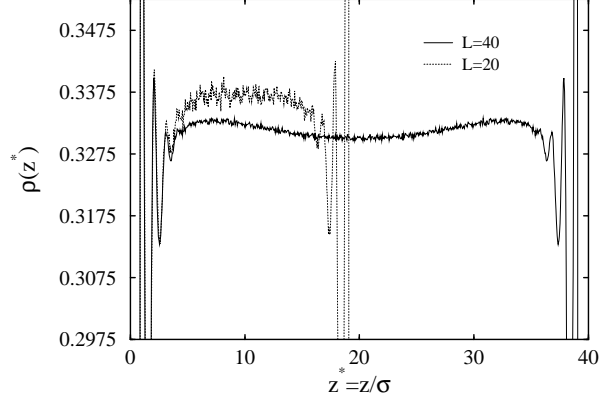
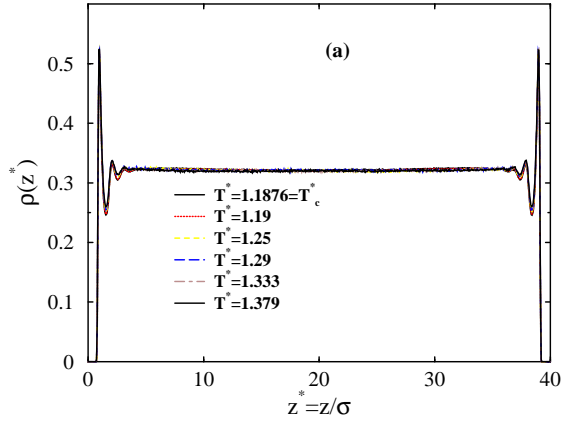


FIG. 3. Critical point density profile  $\rho(z)$  for  $f = 0.653$  for slits of width  $D = 20\sigma$  and  $D = 40\sigma$ . In both cases  $L = 15\sigma$ .



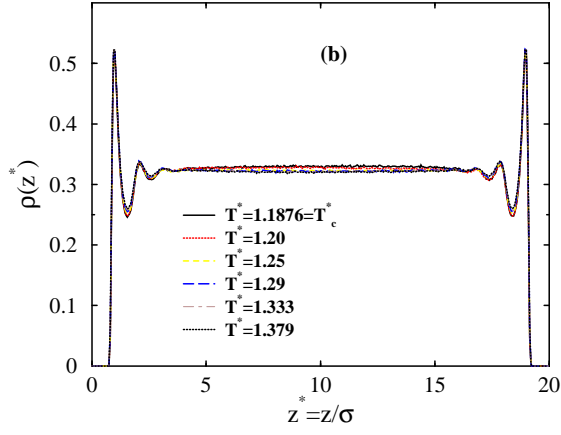


FIG. 4. Density profiles on the critical isochore for  $f = 0.644$ , the 'neutral' wall. (a)  $L = 15\sigma$  and width  $D = 40\sigma$  (b)  $L = 15\sigma$  and width  $D = 20\sigma$ . Note how insensitive the profiles are to the value of  $T^*$

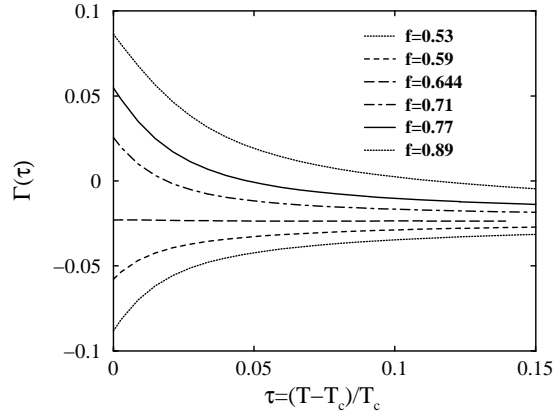


FIG. 5. The adsorption  $\Gamma$ , in units of  $\sigma^2$ , calculated along the critical isochore as a function of reduced temperature  $\tau = (T - T_c)/T_c$  for various values of  $f$ . Results correspond to  $L = 15\sigma$  and width  $D = 20\sigma$ . Note that for the 'neutral' wall  $f = 0.644$ ,  $\Gamma(\tau)$  is constant.

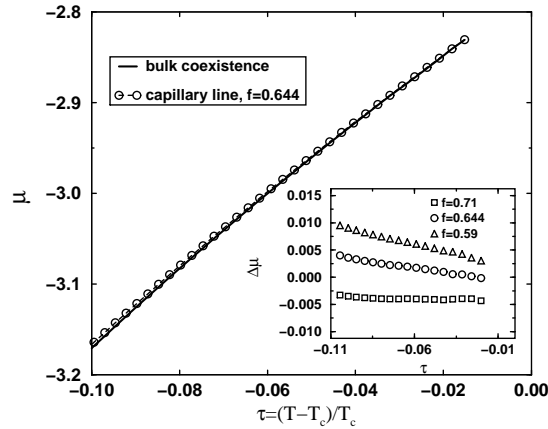


FIG. 6. The chemical potential  $\mu$  (in units of  $k_B T$ ) versus reduced temperature  $\tau$  for capillary condensation in a system of size  $L = 15\sigma$  and width  $D = 20\sigma$  for wall strength  $f = 0.644$ . The thick solid line denotes the bulk coexistence line  $\mu_{cx}$ . The inset displays the difference  $\Delta\mu \equiv \mu - \mu_{cx}$  between the coexistence lines for three values of  $f$ . For  $f = 0.59$ ,  $\mu - \mu_{cx}$  is positive, i.e. there is capillary evaporation.

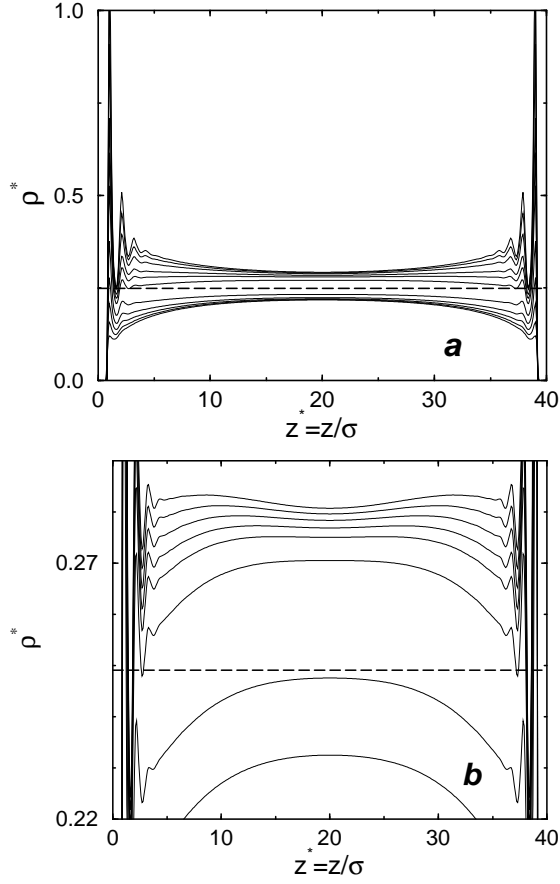


FIG. 7. Critical point density profiles  $\rho(z)$  (in units of  $\sigma^3$ ) for a slit of width  $D = 40\sigma$  and the long-ranged wall-fluid potential  $U_w(z)$  (3.2) obtained using the WDA for several values of the wall strength  $f$ : (a) from top to bottom:  $f = 1.0, 0.9, 0.8, 0.7, 0.65, 0.6, 0.5, 0.4, 0.3, 0.2, 0.1$ . (b) Magnified version for  $f = 0.66, 0.65, 0.64, 0.63, 0.62, 0.6, 0.55$  and  $0.5$ . Note that for  $0.62 \lesssim f \lesssim 0.68$  two smooth maxima, separated by a shallow minimum at the midpoint, arise at distances away from the walls, outside the region where the oscillations due to packing occur. The horizontal dashed line denotes the bulk critical density,  $\rho_c = 0.24912(9)$ .

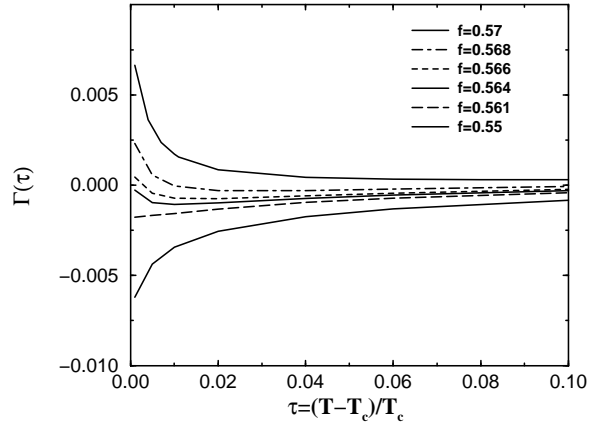


FIG. 8. WDA results for the adsorption  $\Gamma$ , in units of  $\sigma^2$ , calculated for a slit of width  $D = 40\sigma$  along the critical isochore as a function of reduced temperature  $\tau$ , for several values of  $f$ . The wall-fluid potential  $U_w(z)$  (3.2) is long-ranged. Note that the adsorption is very small and only weakly dependent on temperature for the range of values of  $f$  shown here.

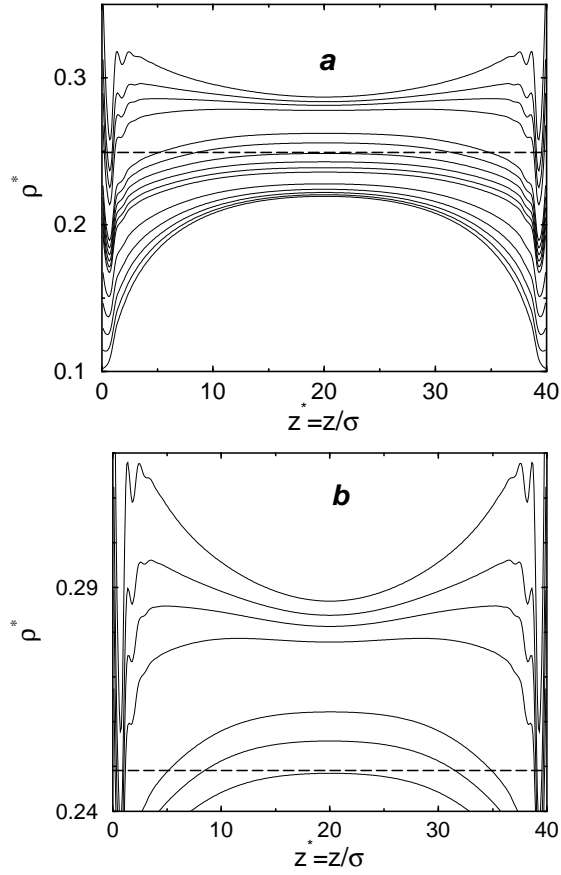
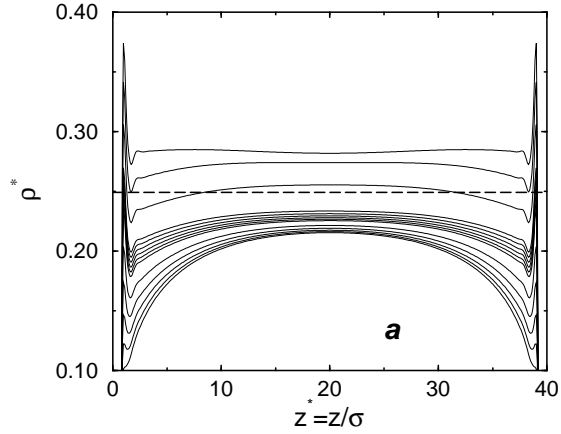


FIG. 9. Critical point density profiles  $\rho(z)$  (in units of  $\sigma^3$ ) for a slit of width  $D = 40\sigma$  and the short-ranged wall-fluid potential  $U_{ws}(z)$  (4.10) obtained using the WDA for several values of the wall strength  $f$ : (a) from top to bottom:  $f = 1.0, 0.9, 0.85, 0.8, 0.7, 0.68, 0.66, 0.64, 0.62, 0.6, 0.5, 0.4, 0.3, 0.2, 0.1$ . (b) Magnified version of (a) for the largest values of  $f$ :  $1, 0.9, 0.85, 0.8, 0.7, 0.68, 0.66$ . The horizontal dashed line denotes the bulk critical density,  $\rho_c = 0.24912(9)$ .





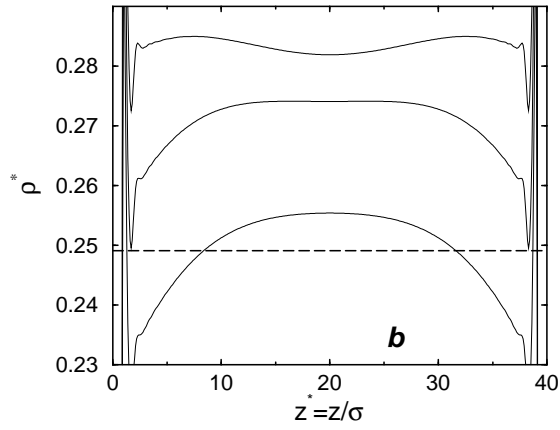


FIG. 10. Critical point density profiles  $\rho(z)$  (in units of  $\sigma^3$ ) for a slit of width  $D = 40\sigma$  and the long-ranged wall-fluid potential  $U_w(z)$  (3.2) obtained using the LDA for the same choice of wall strengths  $f$  as in Fig.9(a). **(b)** Magnified version for  $f = 1, 0.9, 0.8$ . The horizontal dashed line denotes the bulk critical density,  $\rho_c = 0.24912(9)$ .

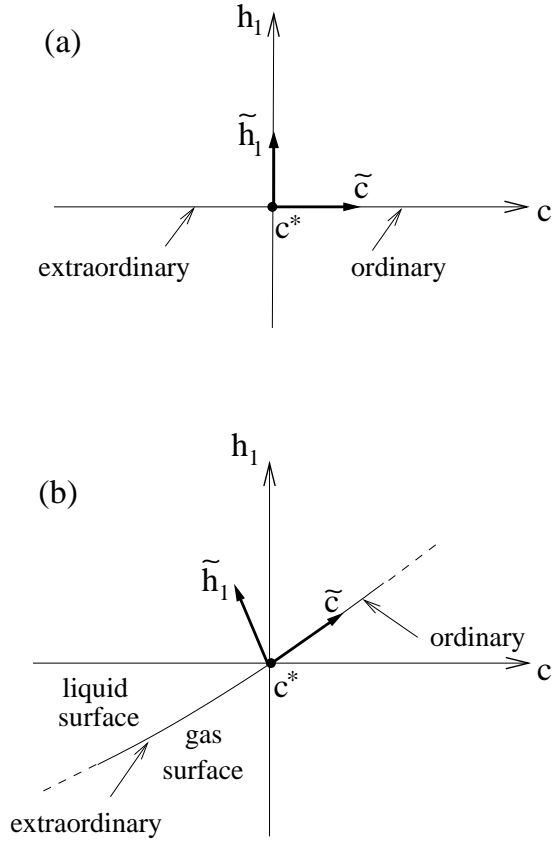


FIG. 11. The form of the surface scaling fields  $\tilde{c}$  and  $\tilde{h}_1$ , for a system at its bulk critical point parameters, as described in the text. **(a)** A model of the Ising symmetry where there is no mixing, so  $\tilde{c} = c$  and  $\tilde{h}_1 = h_1$  **(b)** A fluid system.

[1] K. Binder, in *Phase Transitions and Critical Phenomena* edited by C. Domb and J. L. Lebowitz (Academic Press, London, 1983), vol. 8, p. 1.

- [2] H. W. Diehl, in *Phase Transitions and Critical Phenomena* edited by C. Domb and J. L. Lebowitz (Academic Press, London, 1986), vol. 10, p. 75 and references therein.
- [3] A. J. Bray and M. A. Moore, *J. Phys. A* **10**, 1927 (1977).
- [4] H. W. Diehl, *Int. J. Mod. Phys. B* **11**, 3503 (1997). See also T. W. Burkhardt and H. W. Diehl, *Phys. Rev. B* **50**, 3894 (1994).
- [5] U. Ritschel and P. Czerner, *Phys. Rev. Lett.* **77**, 3645 (1996) and references therein.
- [6] A. Ciach, A. Maciołek, and J. Stecki, *J. Chem. Phys.* **108**, 5913 (1997).
- [7] A. Ciach and U. Ritschel, *Nucl. Phys. B* **489** [FS], 653 (1997).
- [8] P. Czerner and U. Ritschel, *Physica A* **237**, 240 (1997).
- [9] P. Czerner, and U. Ritschel, *Int. J. Mod. Phys. A* **11**, 2765 (1997).
- [10] R. Z. Bariev, *Theo. Math. Phys.* **77**, 1090 (1988).
- [11] R. Konik, A. LeClair and G. Mussardo, *Int. J. Mod. Phys. A* **11**, 2075 (1997).
- [12] R. Chatterjee and A. Zamolodchikov, *Mod. Phys. Lett. A* **9**, 227 (1994).
- [13] A. Maciołek, A. Ciach, and A. Drzewiński, *Phys. Rev. E* **60**, 2887 (1999).
- [14] P. J. Upton, private communication.
- [15] P. J. Upton, *Phys. Rev. Lett.* **81**, 2300 (1998).
- [16] S. B. Kiselev, J. F. Ely and M. Yu. Belyakov, *J. Chem. Phys.* **112**, 3370 (2000) have attempted to interpret the data of M. Thommes, G. H. Findenegg and H. Lewandowski, *Ber. Bunsenges. Phys. Chem.* **98**, 477 (1994) for  $SF_6$  adsorbed, along near-critical isochores, on finely divided graphite adsorbent using a theory which treats  $h_1$  as a field that vanishes (linearly) with  $T - T_c$ . Kiselev et al give no good physical reason as to why  $h_1$  should have this form for this particular system - other than their results; then give a reasonable description of the experimental data! Note that a planar graphite surface would be strongly adsorbing for  $SF_6$ , corresponding to  $h_1 \gg 0$ . These authors take no account of the fact that the substrate is made of colloidal graphite particles which can lead to additional (confining) effects and which is believed to be most relevant for the critical 'depletion' observed in the adsorption measurements - see M. Thommes, G. H. Findenegg and M. Schoen, *Langmuir* **11**, 2137 (1995).
- [17] N. S. Desai, S. Peach, and C. Franck, *Phys. Rev. E* **52** 4129 (1995).
- [18] J.-H. J. Cho and B. M. Law, *Phys. Rev. Lett.* **86**, 2070 (2001).
- [19] W. Fenzl, *Europhys. Lett.* **24**, 557 (1993).
- [20] A useful review of adsorption and wetting phenomena in binary liquid mixtures is given by B. M. Law, *Prog. Surface Science* **66**, 159 (2001).
- [21] B. Nickel, F. Schlesener, W. Donner, H. Dosch and C. Detlefs, *J. Chem. Phys.* **117**, 902 (2002).
- [22] A. M. Ferrenberg and D. P. Landau, *Phys. Rev. B* **44**, 5081 (1991).
- [23] The surface layer magnetisation  $m_1 \sim |\tau|^{\beta_1^{ord}}$  as  $\tau \equiv (T - T_c)/T_c \rightarrow 0^-$ , with  $\beta_1^{ord} \sim 0.8$  for the Ising model in  $d = 3$ . The exponents  $\beta_1^{ord}$  and  $\Delta_1^{ord}$  are related via  $\beta_1^{ord} = (d - 1)\nu - \Delta_1^{ord}$ .
- [24] T. C. Lubensky and M. H. Rubin, *Phys. Rev. B* **12**, 3885 (1975).
- [25] L. Peliti and S. Leibler, *J. Phys. C:Solid State Phys.* **16**, 2635 (1983).
- [26] In the continuum field theory description, careful analysis reveals that near the ordinary transition there is a single relevant surface scaling field  $h_1 \equiv h_1/c^y$ , where  $y$  is a positive exponent [2].
- [27] See, e.g. R. Evans, in *Liquids at Interfaces*, Les Houches Summer School, Session XLVIII (Elsevier, Amsterdam, 1990) p. 3; R. Evans, *J. Phys.:Cond. Mat.* **2**, 8989 (1990).
- [28] D. Frenkel and B. Smit, *Understanding Molecular Simulation*, Academic Press, Boston (1996).
- [29] J. Israelachvili *Intermolecular and Surface Forces*, Academic Press, London (1991).
- [30] A. Maciołek, R. Evans, and N. B. Wilding, *Phys. Rev. E* **60**, 7105 (1999).
- [31] N.B. Wilding, *Phys. Rev.* **E52**, 602 (1995).
- [32] R. Evans, *Adv. Phys.* **28**, 143 (1979).
- [33] U. Marini Bettolo Marconi, *Phys.Rev. A*, **38**, 6267 (1988).
- [34] R. Evans, U. Marini Bettolo Marconi and P.Tarazona, *J.Chem.Phys.*, **84**, 2376 (1985).
- [35] Z. Borjan and P. J. Upton, *Phys. Rev. Lett.* **81**, 4911 (1998).
- [36] R. Evans in *Fundamentals of Inhomogeneous Fluids*, edited by D. Henderson (Dekker, New York, 1992) p. 85.
- [37] P. Tarazona, *Mol. Phys.* **52**, 81 (1984).
- [38] P. Tarazona and R. Evans, *Mol. Phys.* **52**, 847 (1984).
- [39] P. Tarazona, *Phys. Rev. A* **31**, 3672 (1985).
- [40] A. Samborski, J. Stecki and A. Poniewierski, *J. Chem. Phys.* **98**, 8959 (1993).
- [41] J.J. Rehr and N.D. Mermin, *Phys. Rev.* **A8**, 472 (1973).
- [42] Y.C. Kim, M.E. Fisher and E. Luijten, preprint cond-mat/0304032. See this work and references therein for recent progress regarding the role of pressure mixing in the bulk scaling fields.